

Experimental Verification of Models for Determining Dispersion from Attenuation

Ping He, *Senior Member, IEEE*

Abstract—A modified broadband, through-transmission technique is used to compare the accuracy of three models: a nearly local model, a time-causal model, and a discrete minimum phase model, in determining the dispersion from the measured attenuation. By directly measuring the dispersion without first measuring the absolute phase velocity at different frequencies, the new technique eliminates the needs for measuring the speed of sound in the water and the trigger delays in data sampling, and minimizes the uncertainty in determining the phase spectra. Three specimens are used in the study: a block of Plexiglas that has a linear attenuation, a layer of a special rubber compound with an attenuation proportional to $f^{1.38}$, and a phantom made of castor oil that has an attenuation proportional to $f^{1.67}$. For linear attenuation, all three models accurately predict the dispersion. For nonlinear attenuation, the time causal model is shown to be the most accurate model in predicting the dispersion. The nearly local model slightly overpredicts the dispersion in the case of the rubber compound and significantly overpredicts the dispersion in the case of the castor oil. The dispersion determined by the discrete minimum phase model seems to converge to the dispersion determined by the time causal model when the limit of integration is high enough.

I. INTRODUCTION

ULTRASOUND attenuation and (velocity) dispersion are two material properties that are of considerable importance in theoretical acoustics, nondestructive evaluation, and ultrasound tissue characterization [1]–[3]. For a wide variety of materials, including soft tissues, the attenuation increases with frequency according to a power-law relation: $\alpha = \alpha_0|\omega|^y$, where α_0 and y are two material-dependent parameters [4]. Dispersion refers to the phenomenon that the phase velocity of a propagating wave also changes with frequency. Comparing with the attenuation, the magnitude of the dispersion is very small (often less than 1% in the frequency range from 1 to 10 MHz), its frequency dependence is less certain, and its measurement is considered more difficult.

Although many techniques have been developed for measuring the attenuation and dispersion separately [2], [5]–[9], it also has been suggested that these two properties are not independent of each other, and much effort has

been devoted to the development of models that can determine dispersion from attenuation, and vice versa [10]–[14]. The feasibility of such a model is rooted in the theory of analytic functions. If we use $h(t)$ to represent the impulse response of a linear acoustic system, the Fourier transform of $h(t)$ may take the following forms:

$$\begin{aligned} H(\omega) &= R(\omega) + jX(\omega) \\ &= e^{-\alpha(\omega)L} e^{-j\beta(\omega)L} \end{aligned} \quad (1)$$

where $R(\omega)$ and $X(\omega)$ are the real and imaginary parts of the frequency response $H(\omega)$, respectively, $\alpha(\omega)$ is the attenuation coefficient, $\beta(\omega)$ is the propagation constant that is related to the phase velocity V_p by $\beta(\omega) = \omega/V_p(\omega)$, and L is the propagation distance. According to the theory of analytic functions, if $h(t)$ is causal, then $R(\omega)$ and $X(\omega)$ are related to each other by a pair of Hilbert transforms; if $h(t)$ is not only causal but also minimum phase, then $\alpha(\omega)$ and $\beta(\omega)$ are related to each other by Hilbert transforms [15], [16]. When this general theory is applied to the ultrasound measurements, two problems arise. First, the Hilbert transform relations between the attenuation and dispersion are defined in such a way that, in order to obtain the value of one of them at any single frequency, it is necessary to know the values of the other at all frequencies. However, the attenuation is usually measured over a limited frequency range, e.g., from 1 to 10 MHz. The first problem, therefore, is to validate the assumption that the values of α at all other frequencies can be correctly extrapolated from the measured values. The second problem is related to a so-called Paley-Wiener condition which states that, for $A(\omega) = e^{-\alpha(\omega)L}$ to be the Fourier spectrum of a causal function, a necessary and sufficient condition is that the following inequality is satisfied [15]:

$$\int_{-\infty}^{\infty} \frac{|\ln A(\omega)|}{1 + \omega^2} d\omega < \infty. \quad (2)$$

For most materials, the attenuation obeys a power-law frequency dependence $\alpha = \alpha_0|\omega|^y$ where $1 \leq y \leq 2$. For such an attenuation coefficient, the Paley-Wiener condition is not satisfied.

To overcome these problems, several models have been proposed that allow one to determine the dispersion from the local attenuation. In this paper, three models will be discussed. The first model was proposed by O'Donnell *et al.* [10], and is referred to as the nearly local model. The

Manuscript received May 29, 1998; accepted September 29, 1998.

The author is with the Department of Biomedical and Human Factors Engineering, Wright State University, Dayton, OH 45435 (e-mail: phe@cs.wright.edu).

second model was developed by Szabo and is referred to as the time-causal model [13], [14]. Both models require only that the system is linear and causal. For the attenuation obeying a power-law frequency dependence, both models provide closed-form solutions for determining the dispersion from the attenuation. When $y = 1$, the two models predict the same dispersion. When y is increased from 1 to 2, the two models gradually deviate from each other. Besides the data provided in the original paper [10], the accuracy of the nearly local model was experimentally confirmed by Lee *et al.* [9]. However, when both models were tested using the same data, the time-causal model was found more accurate than the nearly local model in predicting the change in wave shape of a broadband pulse passing through a medium [17]. The third model was proposed by Kuc [12] and requires the system to be minimum phase. The Kuc's method [12] numerically calculates the phase function from the measured attenuation by implementing a discrete Hilbert transform algorithm. The method also was found accurate in predicting the change in wave shape of a broadband pulse passing through a medium. In justifying the minimum phase requirement, it was argued that any nonminimum phase transfer function can be written as the product of a minimum phase function and an all-pass function [11], [12]. The all-pass function, however, does not in general have a linear phase. In other words, a real, linear and causal system cannot always be modeled by a minimum-phase system cascaded with another system that produces a pure time delay. Consequently, the minimum phase condition should be considered as an additional assumption that needs to be verified.

The purpose of this paper is to examine the accuracy of the three models by comparing the directly measured dispersion with the dispersion predicted by each model from the measured attenuation. In measuring the dispersion, a modified broadband through-transmission technique is used that requires a minimum number of variables to be measured and eliminates the need for compensating for the phase uncertainty following fast Fourier transform (FFT). The paper is organized as follows. The three models for determining the dispersion from the attenuation are reviewed first. The principle of the dispersion and attenuation measurements is then described, followed by experimental results obtained from three specimens: a block of Plexiglas, a layer of a special rubber compound, and a phantom containing castor oil. This is followed by a discussion.

II. THREE MODELS FOR DETERMINING DISPERSION FROM ATTENUATION

A. Nearly Local Model and Time-Causal Model

By applying the theory of linearity and causality to an acoustic system, and assuming that the attenuation and phase velocity do not change rapidly over the frequency range of interest, O'Donnell *et al.* [10] derived an equation that enables one to calculate the dispersion from the local

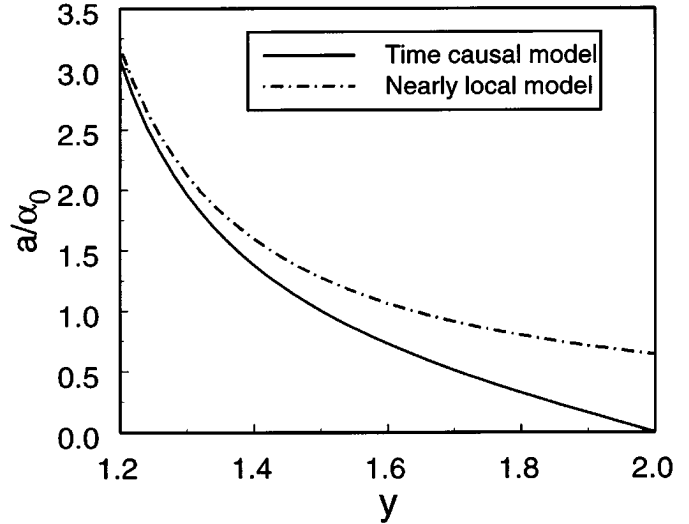


Fig. 1. Comparison of the magnitudes of the dispersion predicted by the time-causal model and by the nearly local model.

attenuation:

$$\frac{1}{V_p(\omega_0)} - \frac{1}{V_p(\omega)} = \frac{2}{\pi} \int_{\omega_0}^{\omega} \frac{\alpha(s)}{s^2} ds \quad (3)$$

where $V_p(\omega_0)$ is the phase velocity at a reference frequency ω_0 . The relations between the dispersion and attenuation based on (3) will be referred to as the nearly local model.

For the attenuation obeying a power-law frequency dependence, Szabo [13] derived a set of time domain lossy wave equations and proposed a new model for determining the dispersion from the attenuation [14]. Szabo's time causal model also incorporates the results obtained independently by Horton [18] and Ochmann and Makarov [19].

When the attenuation is a linear function of frequency ($y = 1$), both the nearly local model and the time causal model predict the same result:

$$\frac{1}{V_p(\omega_0)} - \frac{1}{V_p(\omega)} = \frac{2\alpha_0}{\pi} \ln \frac{\omega}{\omega_0} \quad \text{for } y = 1. \quad (4)$$

For $1 < y \leq 2$, the dispersion predicted by the two models have the same frequency dependence but different magnitudes:

$$\frac{1}{V_p(\omega_0)} - \frac{1}{V_p(\omega)} = a(\omega^{y-1} - \omega_0^{y-1}) \quad \text{for } y > 1 \quad (5)$$

where

$$a = a_n = \frac{2\alpha_0}{\pi(y-1)} \quad \text{for the nearly local model, (6)}$$

and

$$a = a_t = -\alpha_0 \tan(y\pi/2) \quad \text{for the time causal model. (7)}$$

A comparison of the normalized magnitude a/α_0 of the two models is shown in Fig. 1. When y approaches 1, the two models converge. As y approaches 2, the difference

between the two models increases. When $y = 2$, the dispersion vanishes according to the time-causal model and the nearly local model predicts a finite dispersion.

B. Minimum-Phase Model

A minimum-phase model was first proposed by Gurusurthy and Arthur [11] in the continuous time domain for a system having a linear attenuation ($y = 1$). To satisfy the Paley-Wiener condition, the author imposed a high-frequency limit so that the magnitude function does not go to zero faster than an exponential when the frequency goes to infinity. This modification allowed the authors to derive the phase function and obtain an equation that is almost identical to (4). Kuc [12] extended the above work to the discrete time domain. By implementing the Hilbert transform in the discrete time domain, the folding frequency (1/2 sampling frequency) becomes the natural high-frequency limit and the integration of the log-magnitude function is automatically convergent. Although Kuc [12] also considered the case for $y = 1$ only, his method can be easily extended to the nonlinear attenuation. If we extended Kuc's model [12] to a more general attenuation that has a power-law frequency dependence, the phase angle of the minimum-phase system can be determined by the following integration:

$$\beta(\omega) = \frac{\alpha_0}{\omega_s} P \int_{-\frac{\omega_s}{2}}^{\frac{\omega_s}{2}} |\Omega|^y \cot \left[\frac{\pi}{\omega_s} (\Omega - \omega) \right] d\Omega \quad \text{for } 1 \leq y \leq 2 \quad (8)$$

where the symbol P denotes the Cauchy principle value of the integral, and ω_s is the limit of integration [to avoid confusion with the sampling frequency used in data acquisition, we purposely do not call ω_s in (8) the sampling frequency]. After obtaining $\beta(\omega)$ from (8), the dispersion can be calculated as:

$$\frac{1}{V_p(\omega_0)} - \frac{1}{V_p(\omega)} = \frac{\beta(\omega_0)}{\omega_0} - \frac{\beta(\omega)}{\omega}. \quad (9)$$

Because this model does not give a closed-form solution for the dispersion, we will compare the minimum-phase model with the other two models using the experimental data.

III. PRINCIPLE OF DISPERSION AND ATTENUATION MEASUREMENTS

The measurement of attenuation and dispersion using a broadband, through-transmission technique has been described by many authors [5], [7]–[9]. In all these measurements, the absolute phase velocity of the specimen is first determined at a number of frequencies; and the dispersion is then expressed as the change in phase velocity with frequency. In the following section, we describe a modified technique that directly measures the dispersion without first measuring the absolute-phase velocity.

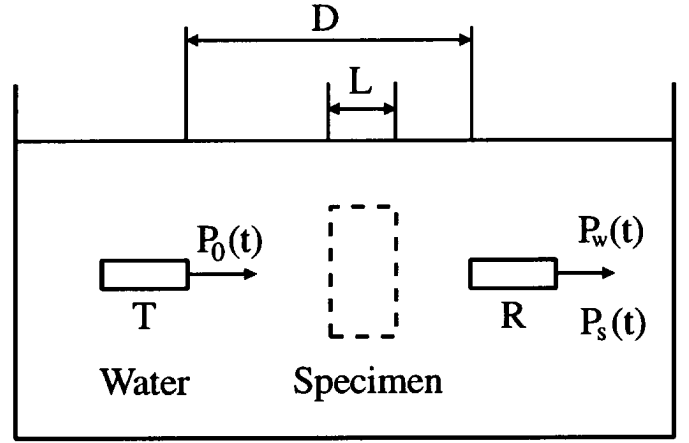


Fig. 2. Simplified experimental setup for dispersion and attenuation measurements.

Fig. 2 shows the simplified experimental setup. Two transducers, separated by a distance D , are placed in a water tank and aligned properly. The transmitting transducer (T) is driven by a pulser, and the receiving transducer (R) is connected to a receiver. The amplified signal is sampled and digitized, and the data are transferred to a computer for processing. For a specimen with a thickness of L , two measurements are performed: one with only a water path and one with the specimen inserted between the two transducers. If we use $P_0(t)$, $P_w(t)$, and $P_s(t)$ to designate the transmitted pulse, the received pulse with the water path only, and the received pulse with the specimen inserted, respectively, the Fourier transforms of $P_w(t)$ and $P_s(t)$ can be found as [9]:

$$\begin{aligned} U_w(\omega) &= A_w(\omega) e^{-j\hat{\varphi}_w(\omega)} \\ &= U_0(\omega) e^{-(\alpha_w + j\beta_w)D} U_r(\omega) \end{aligned} \quad (10)$$

and

$$\begin{aligned} U_s(\omega) &= A_s(\omega) e^{-j\hat{\varphi}_s(\omega)} \\ &= U_0(\omega) e^{-(\alpha_w + j\beta_w)(D-L)} e^{-(\alpha + j\beta)L} T U_r(\omega) \end{aligned} \quad (11)$$

where $U_0(\omega)$, $U_w(\omega)$, $U_s(\omega)$ are the Fourier transforms of $P_0(t)$, $P_w(t)$, $P_s(t)$, respectively; $U_r(\omega)$ is the spectral response of the receiving transducer, $A_w(\omega)$, $A_s(\omega)$, $\hat{\varphi}_w(\omega)$, and $\hat{\varphi}_s(\omega)$ are the amplitude and phase spectra of $U_w(\omega)$ and $U_s(\omega)$, respectively; α_w and α are the attenuation functions, and β_w and β are the propagation constants, of the water and the specimen, respectively; $T = 4z_w z_s / (z_w + z_s)^2$ is the combined transmission coefficient at the two water-specimen interfaces, and z_w and z_s are the acoustic impedance of the water and the specimen, respectively.

The phase spectra $\hat{\varphi}_w(\omega)$ and $\hat{\varphi}_s(\omega)$ in (10) and (11) include the entire propagation delay from the instant when $P_0(t)$ is launched to the instance that $P_w(t)$ or $P_s(t)$ is received. In the actual measurement, the pulses usually are sampled after a certain time delay, as shown in Fig. 3, and the origin of time in calculating the phase spectrum of the

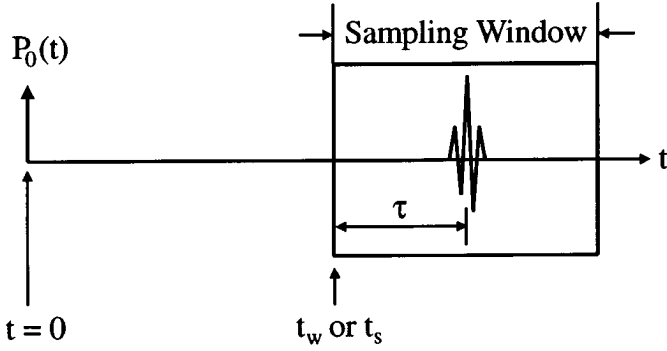


Fig. 3. Temporal relationship among transmitted pulse, $P_0(t)$; received pulse, $P_w(t)$ or $P_s(t)$; and sampling window.

recorded pulse using FFT is the beginning of the sampling window. If we designate the time delays of the sampling windows for $P_w(t)$ and $P_s(t)$ as t_w and t_s , respectively (due to the difference between the sound velocities in the water and in the specimen, t_w may be different from t_s), the phase spectra of the recorded pulses become:

$$\varphi_w(\omega) = \hat{\varphi}_w(\omega) - \omega t_w \quad (12)$$

and

$$\varphi_s(\omega) = \hat{\varphi}_s(\omega) - \omega t_s, \quad (13)$$

respectively. From (10)–(13), we can solve for β :

$$\beta = \frac{\varphi_s(\omega) - \varphi_w(\omega)}{L} + \beta_w + \frac{\omega(t_s - t_w)}{L}. \quad (14)$$

Using the relation $\beta = \omega/V_p(\omega)$, we have:

$$\frac{1}{V_p(\omega)} = \frac{\varphi_s(\omega) - \varphi_w(\omega)}{\omega L} + \frac{1}{c_w} + \frac{(t_s - t_w)}{L} \quad (15)$$

where V_p and c_w are the phase velocities of the specimen and the water, respectively. Equation (15) indicates that, to obtain the absolute phase velocity of the specimen, one needs to know the values of c_w , t_w , and t_s . However, if we directly calculate the change in phase velocity, we have:

$$\frac{1}{V_p(\omega_0)} - \frac{1}{V_p(\omega)} = \frac{\varphi_w(\omega) - \varphi_s(\omega)}{\omega L} - \frac{\varphi_w(\omega_0) - \varphi_s(\omega_0)}{\omega_0 L} \quad (16)$$

where ω_0 is a reference frequency at which the recorded pulse has significant energy. In deriving (16), we assume that the dispersion of the water is negligible [8].

An important feature of (16) is that the terms containing c_w , t_w , and t_s are all cancelled out. This cancellation has two important consequences. First, it simplifies the measurement procedure by reducing the number of variables to be measured. Second, because the actual values of t_w and t_s have no effects on the dispersion, one can arbitrarily move the recorded pulse within the sampling window prior to calculating the phase (a change in τ is equivalent to a change in t_w or t_s). Specifically, a procedure of circularly rotating the pulse to the left is applied

so that the center of the pulse is shifted to the beginning of the sampling window [8]. The purpose of this procedure is to remove the rapid-changing component in the phase spectrum that is associated with the delay τ . After the shifting, the phases of the shifted pulses can be directly used in (16) without the need for time-offset compensation.

The dispersion determined by (16) has a unit of s/m, or the dimension of inverse of velocity. If we use a variable $S(\omega)$ to designate $[1/V_p(\omega_0) - 1/V_p(\omega)]$, then the dispersion also can be expressed by the following dimensionless form:

$$\frac{\Delta V_p(\omega)}{V_0} = \frac{V_p(\omega) - V_p(\omega_0)}{V_p(\omega_0)} = \frac{V_0 S}{1 - V_0 S} \cong V_0 S \quad (17)$$

where $V_0 = V_p(\omega_0)$ is the phase velocity at the reference frequency. In deriving (17), a fact that $|V_0 S| \ll 1$ is utilized. Equation (17) indicates that the two expressions in (16) and (17) differ from each other only by a scale factor V_0 .

By neglecting the attenuation of the water, the attenuation of the specimen can be determined from the amplitude spectra $A_w(\omega)$ and $A_s(\omega)$ [9]:

$$\alpha(\omega) = \frac{1}{L} \ln T + \frac{1}{L} \ln \left[\frac{A_w(\omega)}{A_s(\omega)} \right]. \quad (18)$$

If the unit of L is cm, the unit of α in the above equation is Np/cm. By using the conversion $1 \text{ Np} = 8.686 \text{ dB}$, α can also be expressed in dB/cm.

IV. EXPERIMENTAL PROCEDURE AND RESULTS

Three specimens are used in this study. The first one is a cylindrical block of Plexiglas that has a diameter of 6.3 cm and a thickness (L) of 4.0 cm (the accuracy in determining L is not critical in this study (see Discussion)). The second specimen is a layer of a special rubber compound (No. 35084, BFGoodrich Company, Brecksville, OH) that is used as an acoustic absorber due to its high attenuation and excellent impedance match with the water. The thickness (L) of the specimen is 1.28 cm. The third specimen is a cylindrical phantom made of castor oil (Catalog No: 25,985-3, Aldrich Chemical Company, Milwaukee, WI). To make the phantom, the two ends of a plastic tube (inner diameter = 7.6 cm, $L = 5.5$ cm) are sealed with thin polyethylene film (Glad[®] Cling Wrap, First Brands Corp., Danbury, CT). While the inside of tube is being filled with castor oil, the entire phantom is gradually immersed into the water so that the hydraulic pressures on the two sides of the film are kept nearly equal. The transmitting transducer is Panametrics V309 (5.0 MHz, 13-mm aperture, Waltham, MA), which has a focal length of 8.9 cm. The receiving transducer is Panametrics V384 (3.5 MHz, 6.35-mm aperture) which is nonfocusing. The distance between the two transducers is 18 cm (far field placement) and the water temperature is 22°C. The pulser/receiver used in the

experiment is Panametrics 5052PR with the following settings: energy = 4, damping = 4, H. P. filter = 0.03 MHz. The amplified pulse is digitized by a SONY/TEK 390AD programmable digitizer that has a 10-bit resolution and a sampling frequency of 60 MHz. Each sampling window contains 1,024 samples. The sampled waveforms are averaged 20 times to improve the signal to noise ratio.

In order to ensure the accuracy in attenuation and dispersion measurements, the gain and phase angle of the 5052PR receiver are calibrated between 0.5 MHz and 5 MHz at every increment of 0.5 MHz. The calibration is performed by connecting a sinusoidal signal to the input, then comparing the output signal with the input signal. The measured gains at the 10 discrete frequencies are fitted by a second order curve that is used to correct the amplitude spectra of the recorded pulses prior to calculating the attenuation. The phase of the amplifier is found to be quite linear with frequency. Accordingly, no phase correction is used in the calculation of the dispersion.

To determine the dispersion of the specimen, the phase spectrum of each recorded pulse, $P_w(t)$ or $P_s(t)$, is calculated using the following steps. First, the centroid of the pulse is calculated [8]. The pulse is then circularly shifted to the left so that the centroid is moved to the beginning of the sampling window. The samples originally on the left side of the centroid are wrapped around to the other end of the sampling window. The phase spectrum is then calculated using an FFT algorithm. Additional shift may be applied if the phase spectrum shows discontinuity within the frequency range of interest. Fig. 4 demonstrates the process of phase calculation using the pulses recorded from the castor oil specimen. The dashed line in Fig. 4(a) is the phase spectrum of $P_w(t)$ after its centroid was shifted to the beginning of the sampling window. The phase spectrum is continuous within the frequency range of interest (0.5 to 5 MHz) and no further shifting is needed. However, if we shift the pulse to the left by another two samples (each sample corresponds to $0.01667 \mu\text{s}$), the change in phase spectrum will be further reduced, as shown by the solid line. However, the dashed line in Fig. 4(b), which is the phase spectrum of $P_s(t)$ after its centroid was shifted to the beginning of the sampling window, shows a discontinuity around 4.2 MHz due to phase wrapping. To remove this discontinuity (necessary) and minimize the change in phase angle (not necessary), the pulse is further shifted to the left by seven samples, and the resultant phase spectrum is shown by the solid line in Fig. 4(b). The difference of the two solid lines is plotted in Fig. 4(c). The data shown in this curve are actually used in (16) to calculate the dispersion of the castor oil.

Fig. 5 summarizes the results from the Plexiglas specimen. Fig. 5(a) plots the results of attenuation measurement. The circles represent the values calculated from the amplitude spectra of $P_w(t)$ and $P_s(t)$ using the formula $[\ln(A_w/A_s)]/L$ as shown in (18) with a unit conversion from Np/cm to dB/cm. Because the results show a good linear frequency dependence, the data are fitted with a straight line (solid line) and the two attenuation param-

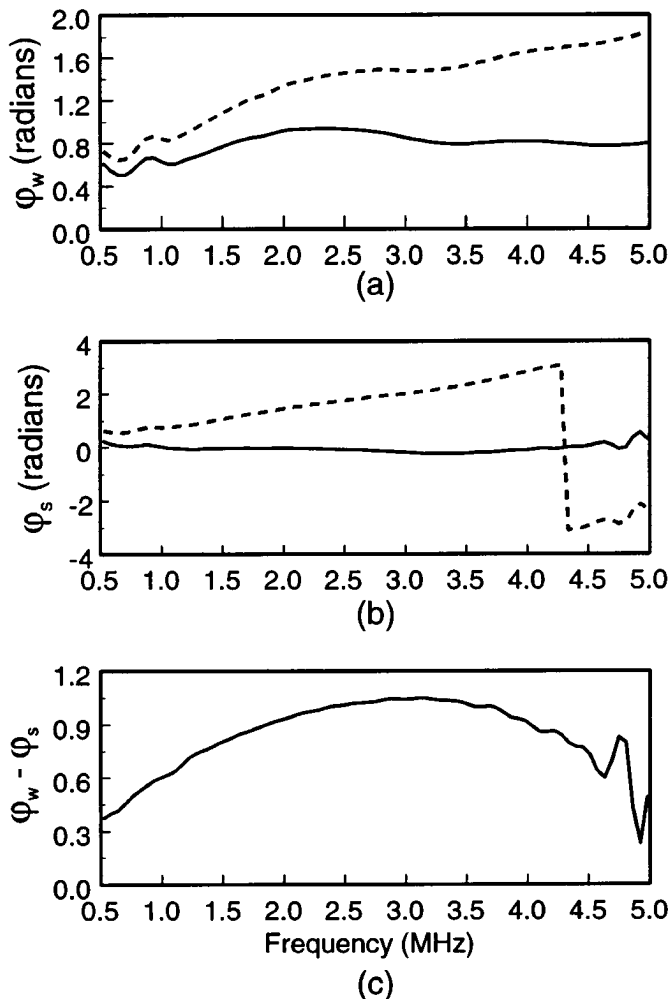


Fig. 4. (a) Dashed line: phase spectrum of $P_w(t)$ after its centroid is shifted to the beginning of sampling window. Solid line: phase spectrum of $P_w(t)$ after further shifting to the left by two samples. (b) Dashed line: phase spectrum of $P_s(t)$ after its centroid is shifted to the beginning of sampling window. Solid line: phase spectrum of $P_s(t)$ after further shifting to the left by seven samples. (c) Difference of the two phase functions (solid lines) shown in (a) and (b).

eters are determined as $y = 1$ and $\alpha_0 = 0.94/(2\pi)$ dB/(cm radians MHz). Fig. 5(b) compares the measured and model predicted dispersions. The circles represent the measured dispersion using (16). The solid line represents the dispersion predicted by the time-causal model and/or nearly local model using (4) with $\alpha_0 = 0.94/(2\pi)$, and the dashed line represents the dispersion predicted by the minimum phase model using (8) and (9) with $f_s = \omega_s/(2\pi) = 60$ MHz, $\alpha_0 = 0.94/(2\pi)$, and $y = 1$. The reference frequency ($f_0 = \omega_0/2\pi$) is 2 MHz. The same reference frequency is used for the other two specimens. As seen in Fig. 5, all three models almost predict identical dispersion that is also very close to the measured dispersion. We also may use Fig. 5(b) to express the relative change in phase velocity $\Delta V_p/V_0$. According to (17), this can be done by simply changing the scale of the ordinate of Fig. 5(b) by a factor of V_0 , which is 2753 m/s for the Plexiglas specimen (V_0 is measured by comparing the time-of-flight of

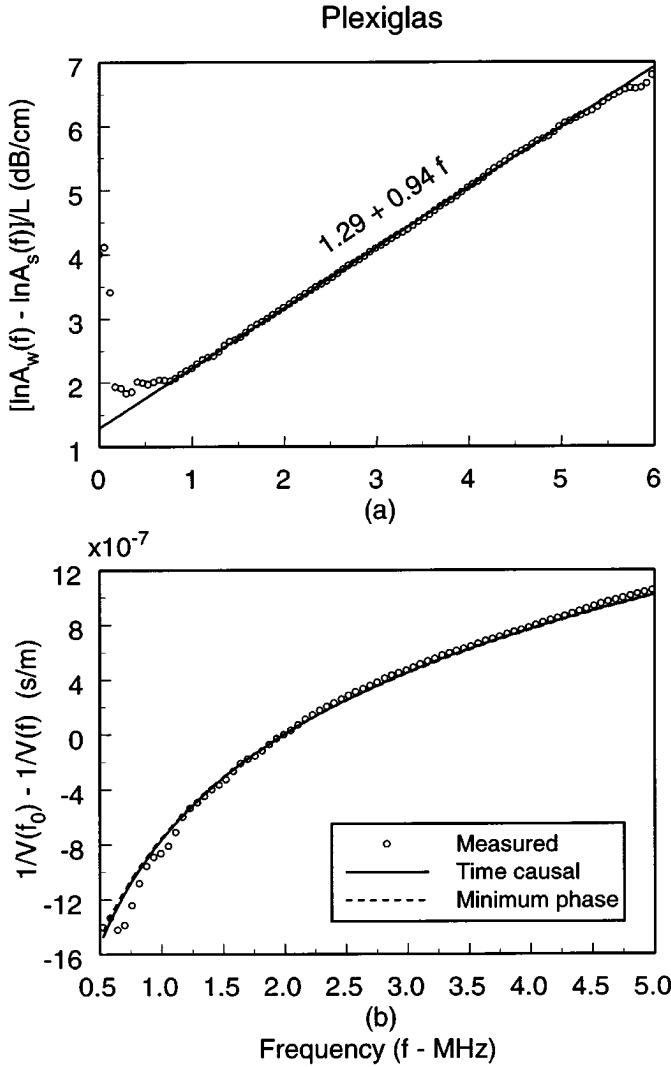


Fig. 5. (a) Attenuation measured (circles) from the Plexiglas specimen, and the fitted least-squares line (solid line). (b) Comparisons of the measured and model-predicted dispersions. The reference frequency is 2 MHz. The measured dispersion corresponds to $\Delta V_p/V_0 \cong -0.38\%$ at 0.5 MHz, and $\Delta V_p/V_0 \cong 0.27\%$ at 5 MHz.

the pulse with and without the specimen inserted between the transmitting and receiving transducers). The measured relative changes in phase velocity at the two ends are: $\Delta V_p/V_0 \cong -0.38\%$ at 0.5 MHz, and $\Delta V_p/V_0 \cong 0.27\%$ at 5 MHz.

Fig. 6 summarizes the results from the rubber compound specimen. The measured attenuation shown in Fig. 6(a) is now fitted with a power curve, and the two parameters are determined as $y = 1.38$ and $\alpha_0 = 7.42/(2\pi)^{1.38}$. Fig. 6(b) compares the measured dispersion (circles) with the dispersions predicted by the three models. The dispersions predicted by the time causal model using (5) and (7) and by the minimum phase model are almost identical, and are also very close to the measured dispersion. The dispersion produced by the nearly local mode using (5) and (6) slightly deviates from the measured dispersion. Using (17) and a measured $V_0 = 1,569$ m/s for the rubber compound, the measured relative changes

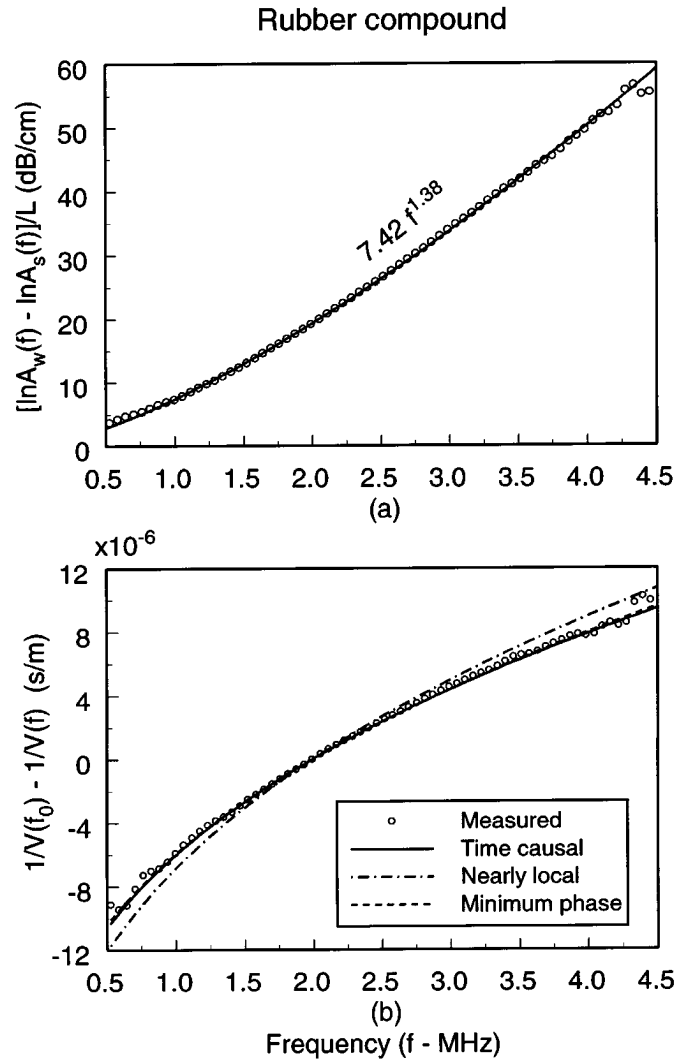


Fig. 6. (a) Attenuation measured (circles) from the rubber compound, and the fitted least-squares curve (solid line). (b) Comparisons of the measured and model-predicted dispersions. The reference frequency is 2 MHz. The measured dispersion corresponds to $\Delta V_p/V_0 \cong -1.6\%$ at 0.5 MHz, and $\Delta V_p/V_0 \cong 1.6\%$ at 4.5 MHz.

in phase velocity are $\Delta V_p/V_0 \cong -1.6\%$ at 0.5 MHz, and $\Delta V_p/V_0 \cong 1.6\%$ at 4.5 MHz. The results from the castor oil are summarized in Fig. 7. The two parameters determined from the attenuation measurement are: $y = 1.67$ and $\alpha_0 = 0.70/(2\pi)^{1.67}$. The dispersion predicted by the time-causal model and the minimum-phase model are close to each other, and closer to the measured dispersion. However, the dispersion predicted by the nearly local model is now significantly different from the measured values. Using (17) and $V_0 = 1,511$ m/s for castor oil, the measured relative changes in phase velocity are $\Delta V_p/V_0 \cong -0.09\%$ at 0.5 MHz, and $\Delta V_p/V_0 \cong 0.12\%$ at 5 MHz.

V. DISCUSSION

We have experimentally compared the accuracy of three models in determining the dispersion from the locally mea-

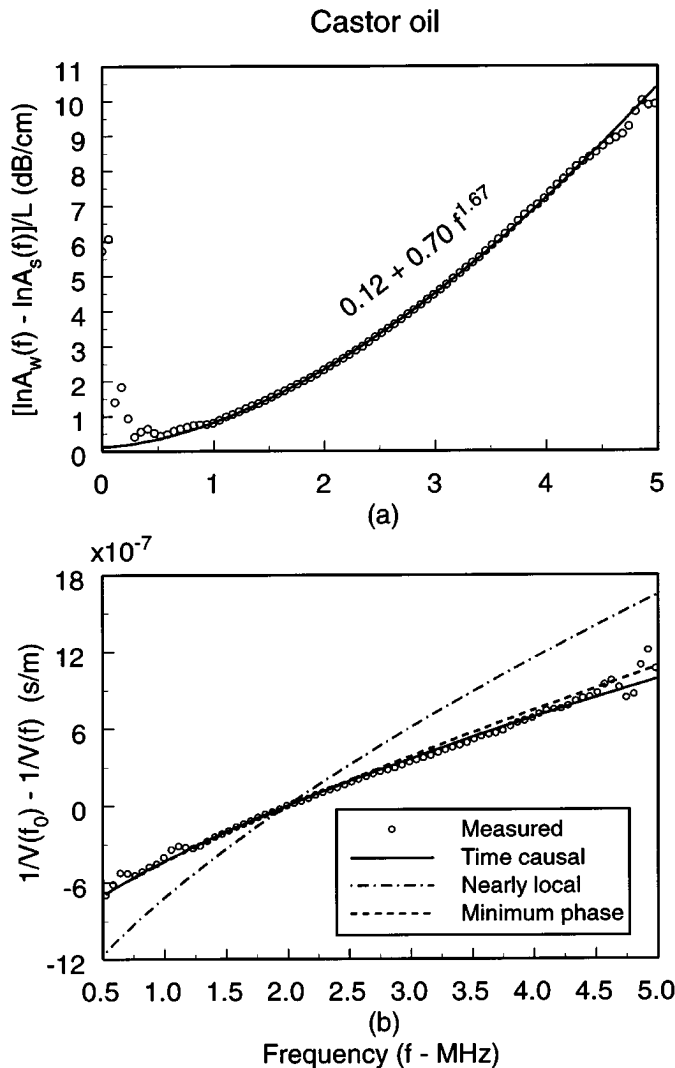


Fig. 7. (a) Attenuation measured (circles) from the castor oil specimen and the fitted least-squares line (solid line). (b) Comparisons of the measured and model-predicted dispersions. The reference frequency is 2 MHz. The measured dispersion corresponds to $\Delta V_p/V_0 \cong -0.09\%$ at 0.5 MHz, and $\Delta V_p/V_0 \cong 0.12\%$ at 5 MHz.

measured attenuation. In measuring the dispersion, a new technique is used that does not give the absolute phase velocity but optimizes the measurement of dispersion in two aspects. First, the technique requires recording only two pulse waveforms: one with and one without the specimen between the transmitting and receiving transducers. The only other variable to be measured is the thickness of the specimen. By eliminating the needs for measuring the sound velocity of the water (c_w) and the trigger delays of the sampling window (t_w and t_s), the associated uncertainties in these measurements also are eliminated. Second, the new technique also eliminates the need for phase unwrapping and the associated $\pm m2\pi$ phase uncertainty [20]. In addition, by formulating the dispersion as shown in (16) rather than using the conventional formula $\Delta V_p = V_p(\omega) - V_p(\omega_0)$ where $V_p(\omega) = c_w/[1 - c_w \Delta\varphi(\omega)/\omega L]$ [20], the comparison among the three models becomes immune to the uncertainty in measuring the thickness of the spec-

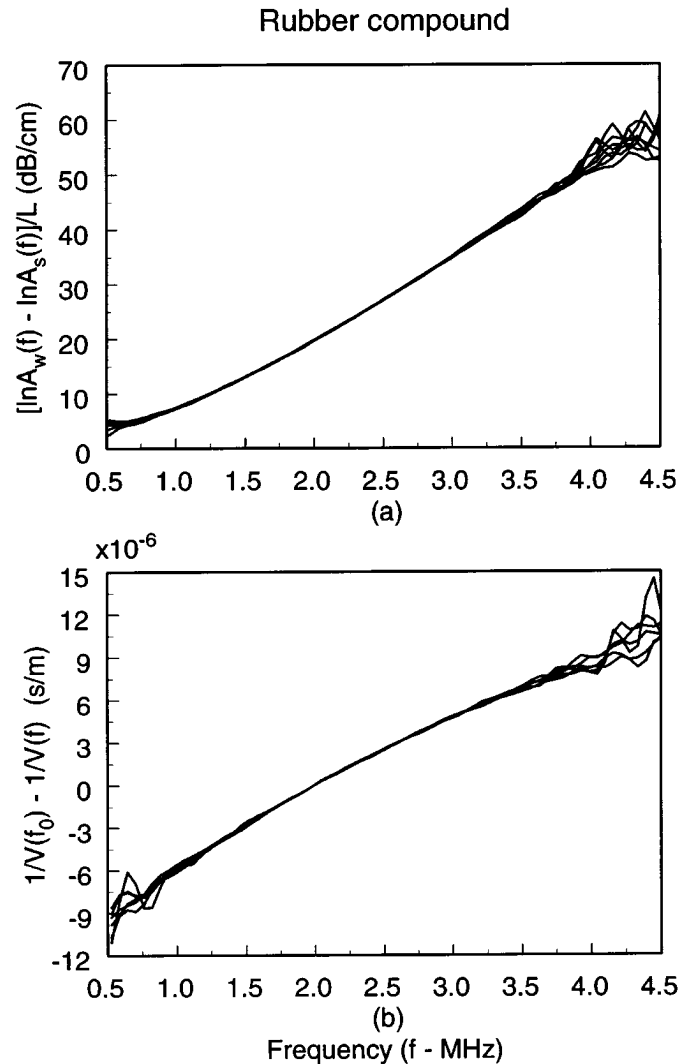


Fig. 8. Attenuation (a) and dispersion (b) measured from the rubber compound under the eight measurement conditions: $D = 12$ cm, 15 cm, 18 cm, and 21 cm with two energy settings on the pulser at each distance.

imen. This is because the dispersion in (16) and the attenuation in (18) are both proportional to $1/L$. In fact, if we multiply the two sides of (5), (16), and (18) by L ; use a new variable $\alpha_0^* = L\alpha_0$ in place of α_0 ; and express the dispersion as $t(\omega_0) - t(\omega) = L/V_p(\omega_0) - L/V_p(\omega)$ (the same way that the speed of a runner is measured in the Olympics), the comparison among the three models can be made even without measuring L . In doing so, we would get exactly the same curves as plotted in Figs. 5 to 7, except for a difference in unit and a scale factor. Considering the fact that the magnitude of dispersion is extremely small, the above advantages make the new technique ideal for the study reported in this paper.

Several authors [21], [22] have reported that the results of attenuation and phase velocity measurement using the ultrasonic spectroscopy technique may be pressure-amplitude dependent and errors can be generated due to the nonlinear distortion. To minimize the error, Wu [22] recommended that effort should be made to keep a shock

parameter $\sigma \leq 0.1$ where σ is defined as:

$$\sigma = \frac{(1 + 0.5B/A)2\pi fp_0x}{\rho_0 c_w^3} \quad (19)$$

where p_0 , ρ_0 , B/A , f , and x are, respectively, the pressure amplitude, density of the water, the nonlinearity parameter of the water, the center frequency of the incident ultrasonic pulse, and the axial distance from the transmitter. Instead of actually measuring the value of σ for the experiment conducted in this study, we systematically changed the value of σ by changing the two variables p_0 and x in (19) and observed the changes in the results of the attenuation and dispersion measurements. To change x , we moved the transmitting transducer to four different locations and kept the receiving transducer and the specimen fixed. To change p_0 , we changed the energy setting of 5052PR pulser/receiver from 4 to 2, which reduces the pulse energy delivered to the transducer from 94 μJ to 36 μJ . The attenuation and dispersion then were measured using the rubber compound specimen under the following eight settings: $D = 12$ cm, 15 cm, 18 cm, and 21 cm with two energy settings at each distance. The resultant eight attenuation curves are superposed in Fig. 8(a), and the eight dispersion curves are superposed in Fig. 8(b). These figures indicate that the measurement conditions used in this study do not evoke nonlinear distortion, and the results of attenuation and dispersion measurements are quite stable and should be reliable.

Results from this study verify the accuracy of the time-causal model proposed by Szabo [14]. For both linear and nonlinear attenuation, the time-causal model predicts the dispersion accurately. The dispersion determined by the nearly local model is exaggerated when the power index y is larger than one, and the degree of exaggeration increases as y is increased from 1.38 to 1.67, as shown in Figs. 6 and 7. This trend is in agreement with the curves shown in Fig. 1. The above observation also agrees with an earlier report [17] in that the time-causal model is found more accurate than the nearly local model in predicting the wave shape change of an ultrasound pulse passing through a specimen. However, Lee *et al.* [9] measured the attenuation and dispersion of two specimens of polyurethane and reported a good agreement between the measured dispersion and the dispersion predicted by the nearly local model. The attenuation coefficients of the two specimens used in their experiment have a degree of nonlinearity ($y = 1.707$ and 1.668, respectively) which is similar to that of the castor oil specimen ($y = 1.67$) used in this study. With such a large value of y , the dispersion predicted by the nearly local model is significantly different from that predicted by the time-causal model, as shown in Fig. 1. Based on the fact that these authors [9] only tested the nearly local model, a possible explanation for the apparent discrepancy between their results and the results reported in this study is that the technique used by these authors [9] may not be sensitive enough to signalize the deviation of the model prediction from the measured dispersion. With the improved accuracy and precision, the technique used in

this study not only shows clear differences among the measured dispersion and the dispersions predicted by different models in the case of $y = 1.67$ (Fig. 7), but also detects more subtle differences in the case of $y = 1.38$ (Fig. 6).

An interesting observation is that the dispersion predicted by the minimum phase model is very close to the prediction made by the time causal model. For the Plexiglas ($y = 1$) and rubber compound specimens ($y = 1.38$), the differences between the two models are almost imperceptible. For the castor oil specimen ($y = 1.67$), the minimum phase model slightly overpredicts the dispersion. It should be pointed out that the dispersion determined by (8) and (9) is dependent on the limit of integration ω_s used for calculating the phase. In obtaining the results shown in Figs. 5, 6, and 7, a limit of integration $f_s = \omega_s/(2\pi) = 60$ MHz was used. If the f_s is increased from 60 to 90 MHz, 120 MHz, and then 150 MHz, the curve corresponding to the minimum phase model in Fig. 7 gradually moves toward the curve corresponding to the time-causal model. At 120 MHz, the distance between the two curves is more than halved. The curves in Figs. 5 and 6 also are further merged into the curves corresponding to the time-causal model. This observation suggests that the minimum-phase model may approach the time-causal model asymptotically when the limit of integration keeps increasing (in doing so, the Kuc's [12] discrete minimum-phase model approaches to the continuous time domain minimum-phase model proposed by Gurumurthy and Arthur [11]). In Kuc's original paper, it was shown that the accuracy of the impulse response of a block of Plexiglas determined by the minimum-phase model gradually improves when the limit of integration is increased from 10 to 20 MHz, 50 MHz, and 100 MHz (Fig. 6 of ref. [12]). By combining the Kuc's [12] observation and the results obtained in this study, we may reach the following conclusions. First, because the minimum-phase model and the time-causal model are derived independently, the fact that the results from the two models are in excellent agreement with each other (and also in excellent agreement with the experimental data) validates both models. Second, for attenuation obeying a power-law frequency dependence, the time-causal model is the choice for determining the dispersion from the attenuation because the minimum-phase model does not have a closed-form solution, and the computation of discrete Hilbert transform is very time consuming. Third, as stated previously, that, in theory, a causal but nonminimum phase transfer function cannot in general be written as the product of a minimum phase function and an all-pass function that also has a linear phase. The results from this study, however, suggest that a linear acoustic system, or at least for the three specimens used in this study, can indeed be modeled by a minimum-phase system cascaded with another system that produces a pure time delay.

A question may arise: if the dispersion can be determined accurately from the measured attenuation, is there still a need for measuring the dispersion? The answer is yes. First, using the technique presented in this paper, the

measurement of the dispersion is as simple as the measurement of the attenuation. In fact, both the attenuation and dispersion can be determined by the same pair of recorded pulses. Second, because the measurements of attenuation and dispersion are two independent processes that the accuracy of each measurement is affected by difference factors, by measuring both the attenuation and dispersion, the accuracy of the overall measurement can be improved. Noticing that, for an attenuation having a power-law frequency dependence, the measurement of attenuation and dispersion reduces to the estimation of two parameters: α_0 and y . By measuring both attenuation and dispersion, the two parameters can be determined more accurately than by measuring the attenuation only. Finally, the time-causal model is only applied to a linear system. By measuring both the attenuation and dispersion, one may reveal possible nonlinearity of the underlying process. For example, in an experiment with highly porous cancellous bone, Droin *et al.* [23] reported a systematic deviation between the measured dispersion and the one predicted by the local form of the Kramers-Kronig relationship. The heterogeneity may have a profound effect on wave propagation, and mechanisms other than frequency dependent attenuation may have to be invoked to describe the dispersion in cancellous bone.

REFERENCES

- [1] R. L. Weaver and Y. H. Pao, "Dispersion relations for linear wave propagation in homogeneous and inhomogeneous media," *J. Math. Phys.*, vol. 22, pp. 1909–1918, 1981.
- [2] R. A. Kline, "Measurement of attenuation and dispersion using an ultrasonic spectroscopy technique," *J. Acoust. Soc. Amer.*, vol. 76, pp. 498–504, 1984.
- [3] J. C. Bamber and C. R. Hill, "Acoustic properties of normal and cancerous human liver—I. Dependence on pathological condition," *Ultrason. Med. Biol.*, vol. 7, pp. 121–133, 1981.
- [4] P. N. T. Wells, "Review: Absorption and dispersion of ultrasound in biological tissue," *Ultrason. Med. Biol.*, vol. 1, pp. 369–376, 1975.
- [5] A. C. Kak and K. A. Dines, "Signal processing of broadband pulsed ultrasound: Measurement of attenuation of soft biological tissues," *IEEE Trans. Biomed. Eng.*, vol. BME-25, pp. 321–344, 1978.
- [6] E. L. Carstensen, "Measurement of dispersion of velocity of sound in liquids," *J. Acoust. Soc. Amer.*, vol. 26, pp. 858–861, 1954.
- [7] W. Sachse and Y. H. Pao, "On the determination of phase and group velocities of dispersive waves in solids," *J. Appl. Phys.*, vol. 49, pp. 4320–4327, 1978.
- [8] S. I. Rokhlin, D. K. Lewis, K. F. Graff, and L. Adler, "Real-time study of frequency dependence of attenuation and velocity of ultrasonic waves during the curing reaction of epoxy resin," *J. Acoust. Soc. Amer.*, vol. 79, pp. 1786–1793, 1986.
- [9] C. C. Lee, M. Lahham, and B. G. Martin, "Experimental verification of the Kramers-Kronig relationship for acoustic waves," *IEEE Trans. Ultrason., Ferroelect., Freq. Contr.*, vol. 37, pp. 286–294, 1990.
- [10] M. O'Donnell, E. T. Jaynes, and J. G. Miller, "Kramers-Kronig relationship between ultrasonic attenuation and phase velocity," *J. Acoust. Soc. Amer.*, vol. 69, pp. 696–701, 1981.
- [11] K. V. Gurumurthy and R. M. Arthur, "A dispersion model for the propagation of ultrasound in soft tissue," *Ultrason. Imaging*, vol. 4, pp. 355–377, 1982.
- [12] R. Kuc, "Modeling acoustic attenuation of soft tissue with a minimum-phase filter," *Ultrason. Imaging*, vol. 6, pp. 24–36, 1984.
- [13] T. L. Szabo, "Time domain wave equations for lossy media obeying a frequency power law," *J. Acoust. Soc. Amer.*, vol. 96, pp. 491–500, 1994.
- [14] —, "Causal theories and data for acoustic attenuation obeying a frequency power law," *J. Acoust. Soc. Amer.*, vol. 97, pp. 14–24, 1995.
- [15] A. Papoulis, *The Fourier Integral and Its Application*. New York: McGraw-Hill, 1962, pp. 192–217.
- [16] A. V. Oppenheim and R. W. Schaffer, *Digital Signal Processing*. Englewood Cliffs, NJ: Prentice-Hall, 1975, pp. 337–353.
- [17] P. He, "Simulation of ultrasound pulse propagation in lossy media obeying a frequency power law," *IEEE Trans. Ultrason., Ferroelect., Freq. Contr.*, vol. 45, no. 2, pp. 114–125, 1998.
- [18] C. W. Horton, Sr., "Dispersion relationships in sediments and sea water," *J. Acoust. Soc. Amer.*, vol. 55, pp. 547–549, 1974.
- [19] M. Ochmann and S. Makarov, "Representation of the absorption of nonlinear waves by fraction derivatives," *J. Acoust. Soc. Amer.*, vol. 94, pp. 3392–3399, 1993.
- [20] J. Mobley, J. N. Marsh, C. S. Hall, M. S. Hughes, G. H. Brandenburger, and J. G. Miller, "Broadband measurements of phase velocity in Alunex® suspensions," *J. Acoust. Soc. Amer.*, vol. 104, pp. 2145–2153, 1998.
- [21] B. Zeqiri, "Errors in attenuation measurements due to nonlinear propagation effects," *J. Acoust. Soc. Amer.*, vol. 91, pp. 2585–2593, 1992.
- [22] J. Wu, "Effects of nonlinear interaction on measurements of frequency-dependent attenuation coefficients," *J. Acoust. Soc. Amer.*, vol. 99, pp. 3380–3384, 1996.
- [23] P. Droin, P. Laugier, and G. Berger, "Ultrasonic attenuation and dispersion in highly porous cancellous bone in the frequency range 200–600 KHz," *Ultrason. Imaging*, vol. 19, pp. 55–56, 1997 (abstr.).



Ping He (SM'85) received the B.S. degree in physics in 1968 from Fudan University, Shanghai, China, and the M.S. and Ph.D. degrees in biomedical engineering in 1981 and 1984, respectively, from Drexel University, Philadelphia, PA.

He was a Research Fellow in the Biodynamic Research Unit, Mayo Clinic, from 1984 to 1985, where he worked on ultrasonic tissue characterization. Since 1985, he has been with the Department of Biomedical and Human Factors Engineering, Wright State University, Dayton, OH, where he is currently an associate professor.

Dr. He's research interests are in medical imaging, biological signal processing, and bioinstrumentation. He is a senior member of IEEE, and a member of AIUM and ASEE.